Mem. S.A.It. Vol. 79, 432

Memorie della

Mass loss in Population II giant stars

Livia Origlia

Istituto Nazionale di Astrofisica – Osservatorio Astronomico di Bologna, via Ranzani 1, I-40127 Bologna, Italy, e-mail: livia.origlia@oabo.inaf.it

Abstract. In the first part of this review I will summarize our current knowledge of mass loss in Population II giants in terms of observational constraints and modeling. In the second part I will briefly discuss first, new results from our SPITZER survey of a carefully chosen sample of 17 Galactic Globular Clusters, spanning a wide metallicity range from about one hundredth up to almost solar and with different Horizontal Branch morphology.

Key words. Stars: mass loss – Stars: Population II – Galaxy: globular clusters

1. Introduction

Mass loss (ML) is a critical parameter in any stellar evolution modeling. Despite its importance, satisfactory empirical determinations as well as a comprehensive physical description of the involved processes are still lacking. This is especially true for Population II Red Giant Branch (RGB) and Asymptotic Giant Branch (AGB) stars.

The astrophysical impact of ML in Population II giants is huge and affects not only the stellar evolution modeling but also related subjects, like for example the UV excess in ellipticals or the interaction between the cool intracluster medium and hot halo gas.

There is so much indirect but quantitative evidence for ML during the giant branches evolution, namely the Horizontal Branch (HB) morphology and the 2^{nd} parameter problem, the pulsational properties of RR Lyrae, the absence of AGB stars brighter than the RGB tip and the masses of White Dwarfs (WDs) in globular clusters (GCs) (Rood 1973; Fusi Pecci & Renzini 1975, 1976; Renzini 1977; Fusi Pecci et al. 1993; Castellani & Castellani 1993; D'Cruz et al. 1996; Hansen 2005; Kalirai et al. 2007).

The state of the art of our knowledge of ML in Population II giants can be schematized as follows. There is a lack of any empirical law directly calibrated on Population II giants. Indeed, only a few, sparse estimates of ML for giants on the brightest portion of the RGB and AGB exist. Also ML timescales, driving mechanisms, dependence on stellar parameters and metallicity are still open issues, implying little theoretical or observational guidance on how to incorporate ML into models.

Without any better recipe, models of stellar evolution incorporate ML by using analytical ML formulae calibrated on Population I bright giants, the first and most used being the Reimers (1975a,b) formula, extrapolated towards lower luminosity by also introducing a free parameter η (typically 0.3), to account for a somewhat less efficient ML along the RGB. A few other formulae, which are variants of the Reimers one, have been proposed in the subsequent years (Mullan 1978;

Send offprint requests to: L. Origlia

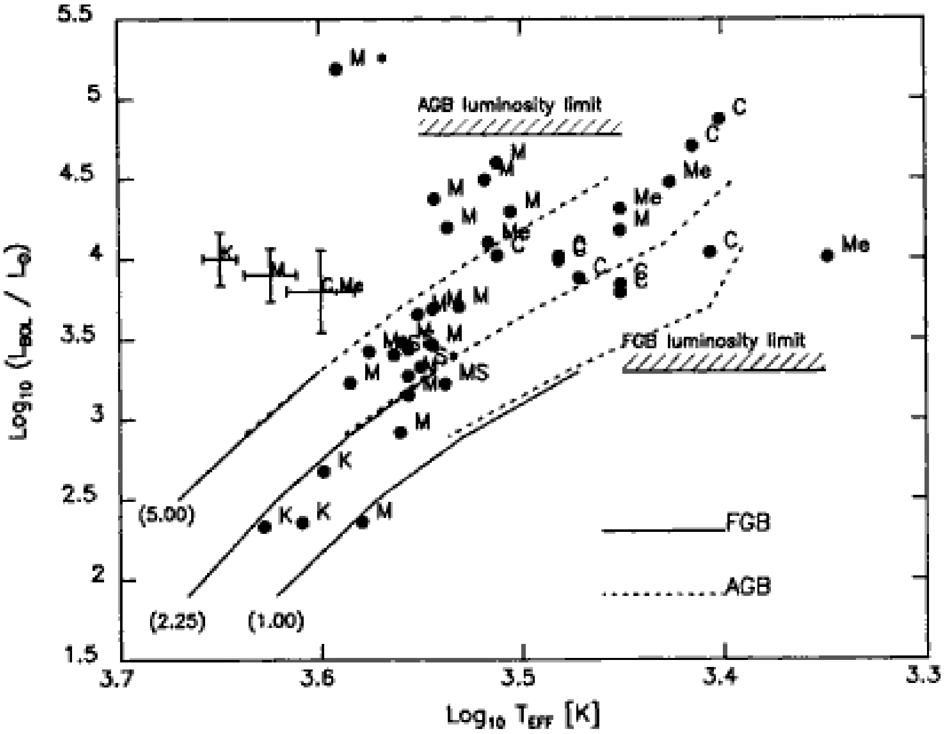

Fig. 1. H-R diagram of stars on the first (RGB) and second (AGB) ascents of the giant branch. Theoretical evolutionary tracks for progenitor masses between 1 and 5 $M_{\odot}$ are also plotted for reference. From Judge (1991).

Goldberg 1979; Judge 1991). More recently, Catelan (2000) revised these formulae by using a somewhat larger database of giant stars, and Schroeder & Cuntz (2005) propose a new formula which explicitly includes a dependence from all the stellar parameters. However, the Judge (1991) database used by Catelan (2000) (see Fig.1) still counts only 20-30 giants, the majority being AGB stars. So, empirical estimates of ML rates in low-mass giants along the entire RGB extension is definitely urgent.

2. Mass loss diagnostics

There are two major diagnostics of ML in giant stars: the detection of outflow motions in the outer regions of the stellar atmosphere or the detection of circumstellar envelopes (CSE) at much larger distances from the star.

2.1. Chromospheric lines

The investigation of chromospheric lines in giants stars with possible emission wings (see Fig.2) started in the '80.

Gratton (1983), Cacciari & Freeman (1983), Gratton et al. (1984) measured Hα emission in old, bright giants near the RGB tip, members of Galactic globular and open clusters. They find Hα emission in a significant fraction of them and, by using the simple recombination model by Cohen (1976), they estimated average $dM/dt \approx 10^{-8} M_{\odot}\,yr^{-1}$ ML rates. However, Dupree et al. (1984); Dupree (1986) argued that the Hα wings could naturally arise in a static stellar chromosphere.

About one decade later, several authors (e.g. Dupree et al. 1992, 1994; Lyons et al. 1996; Smith et al. 2004; Cacciari et al. 2004;

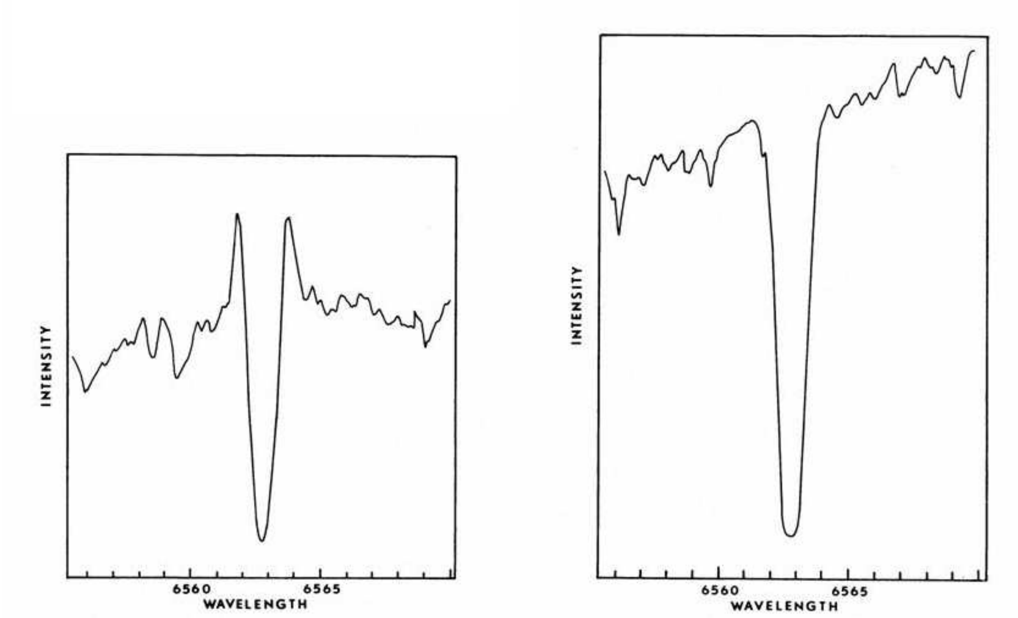

Fig. 2. Comparison between a star with Hα emission wings (left panel) and without (right panel). From Gratton (1983).

Mauas, Cacciari & Pasquini 2006) investigated the possible presence of profile asymmetries and coreshifts in a large number of chromospheric lines, by means of high resolution spectroscopy over a wide spectral range, from UV (MgII h,k λ2800 Å) to optical (CaII K, NaI D, Hα) and IR(HeI λ10830.3 Å). These line asymmetries and coreshifts can be accounted for only by an active chromosphere and/or mass outflows. They find typical velocity fields of 10-20 km/s and $dM/dt \approx 10^{-9} M_{\odot}\,yr^{-1}$ ML rates. However, it must be noted that these ML rates are about one order of magnitude lower than previously estimated from Hα emission wings and predicted by the Reimers or the Schroeder & Cuntz (2005) formulae.

The difficulty of converting the chromospheric line diagnostics into ML rates is certainly related to modeling uncertainties, due for example the lack of any detailed knowledge of the structure and excitation mechanism of the wind region. However, it is also clear that the outflow region traced the chromospheric lines is still too close to the star, to sample the bulk of ML, likely concentrated at larger distances. Hence, the chromospheric line method seems more effective in tracing the region of wind formation and acceleration, rather than most the outflow. Finally, it must be recalled that even with 8m-class telescopes it is at best expensive and often impossible to obtain high resolution, high S/N spectra of Population II giants along the entire RGB extension.

2.2. Circumstellar dust

A CSE around a cool giant can be detected by measuring IR dust emission, linear polarization, microwave CO emission and radio OH masers. However, CSE of low-mass giants have intrinsically low surface brightness. Far IR and radio receiver have neither sufficient spatial resolution nor sensitivity to study Population II CSE in dense stellar fields. Linear polarization, intrinsically well below 1% is also hardly measurable. Hence, array photometry in the 3-20 micron region re-

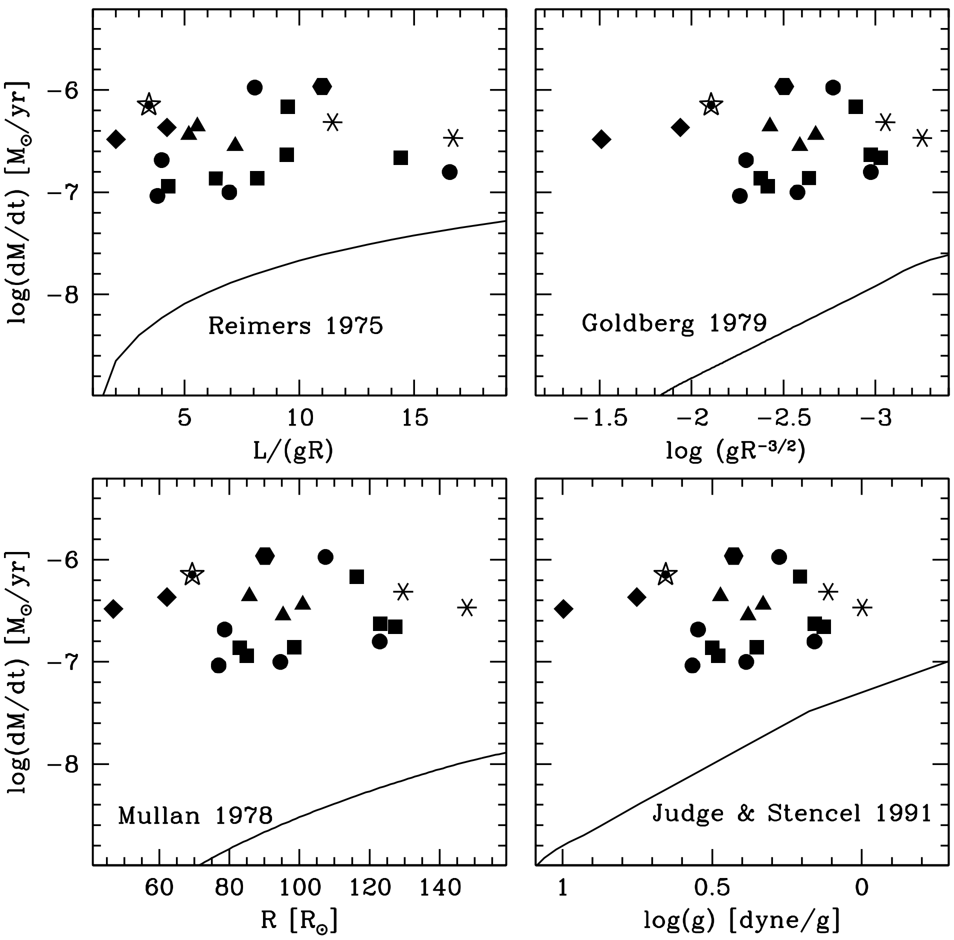

Fig. 3. Mass loss rates for GC giant stars with dust excess, as observed with ISOCAM, as a function of different stellar parameters. Different empirical laws by Reimers (1975a,b); Mullan (1978); Goldberg (1979); Judge (1991) recently revised by Catelan (2000), are shown for comparison. From Origlia et al. (2002).

mains the most effective diagnostics to detect Population II CSE.

Mid-IR observations have the advantage of sampling an outflowing gas fairly far from the star (typically, tens/hundreds stellar radii). Such gas left the star a few decades previously, hence the inferred ML rate is also smoothed over such a timescale. In late '80s, first measurements of dust excess in GC giants by means of mid IR photometry from the ground (Frogel & Elias 1988) and with IRAS (Gillet et al. 1988; Origlia et al. 1996) became available, although the spatial resolution of these detectors was insufficient to properly resolve most of the stars.

A decade later, the ISO satellite allowed new observations, but still limited in spatial resolution and sensitivity. A few bright

AGB stars in 47 Tuc have been measured by (Ramdani & Jorissen 2001), finding dust excess in 2 objects only. Our group performed a deep survey with ISOCAM of 6 massive Galactic GCs (Origlia et al. 2002), namely 47 Tuc, NGC 362, omega Cen, NGC 6388, M15 and M54, in the 10 micron window. From a combined physical and statistical analysis, our ISOCAM study provided ML rates (see Fig.3 and frequency. We found that *i)* the largest ML occurs near the very end of the RGB evolutionary stage and is episodic, *ii)* typical rates are in the range $10^{-7} < dM/dt < 10^{-6} M_{\odot}\,\mathrm{yr}^{-1}$, *iii)* the modulation timescales must be greater than a few decades and less than a million years, and *iv)* there is evidence for dusty shells at even the lowest metallicities. However, our ISOCAM survey suffered from two significant limitations. The small sample of observed clusters and the low number of detected giants allowed us to reach only weak conclusions on the ML dependence on metallicity and HB morphology. Further, the modest spatial resolution and sensitivity compromised our ability to measure lower ML rates near the RGB tip and made it impossible to explore ML much below the RGB tip.

3. The SPITZER era

The advent of SPITZER with its mid IR camera IRAC has opened a new window in the study of CSE around Population II giants. Indeed, the IRAC bands between 3.6 and 8 μm are effective in detecting warm dust with spatial resolution good enough to resolve most of the GC giants.

Boyer et al. (2006) presented the results from SPITZER observations of the M15 core region. They detected ≈20 dusty AGB and post-AGB stars and found ≈ 10^{-3} $M_{\odot}$ intracluster dust accumulated within 1 Myr.

Our group, has been granted 26 hr with IRAC onboard SPITZER (program ID #20298), to map the central region of 17 Galactic GCs with different metallicity and HB morphology, down to the HB level. Complementary near-IR and UV photometry have been also secured, to properly identify the stellar counterparts and characterize both the red and the blue sequences. More details on the survey and data reduction can be found in Fabbri et al. (this conference). First results for 47 Tuc have been recently published (Origlia et al. 2007) and summarized as follows. In the central $9' \times 5'$ 93 giants show $(K\text{-}8)_0$ color excess at a 3σ level. The seven 47 Tuc stars which showed dust excess in our ISOCAM survey have been also detected by SPITZER and confirmed as dusty stars. Among the SPITZER dusty giants, four are known long period variables (V1, V4, V6, & V8 in Clement et al. (2001)) and an other 17 stars are classified as AGB stars by Beccari et al. (2006). Hence, the remaining 74 giants have been classified as true RGB dusty stars. In order to obtain the ML rates we use our modified version of the DUSTY code (Ivezić, Nenkova & Elitzur 1999; Elitzur & Ivezić 2001), to compute the emerging spectrum and dust emission at the IRAC wavelengths. While radiation pressure acting on dust might plausibly drive winds in luminous, metal rich red giants (Willson 2000), the GC stars are generally neither luminous nor metal rich enough for this mechanism to be efficient. Hence we run the DUSTY code under the general assumption of an expanding envelope at constant velocity $v_{\rm exp}$ with a density profile $\eta \propto r^{-2}$. We adopt a gas to dust ratio $\delta \approx 1/Z \approx 200$, where Z is the cluster metallicity, and an expansion velocity $v_{\rm exp} = 10\ \mathrm{km\,s^{-1}}$. The latter is the average expansion velocity measured in luminous, low mass giants (see e.g. Netzer & Elitzur 1993) which ranges between a few and ≈ 20 kms^{-1}. For the dusty stars in 47 Tuc sampled by our SPITZER survey, Fig. 4 shows the inferred ML rates as a function of *i)* the observed $(K-8)_0$ color, *ii)* the bolometric magnitude and *iii)* the normalized luminosity. The ML rate increases with increasing color excess and stellar luminosity. Also, the bulk of the ML along the RGB should occur above the HB level. The provisional empirical law based on such a first set of observations gives:

$$dM/dt = C \times 4 \times 10^{-10} \times (L/gR)^{0.4}_{\odot} \qquad (1)$$

where

$$C = (\delta/200)^{0.5} \times (v_{\rm exp}/10) \times (\rho_{\rm g}/3) \qquad (2)$$

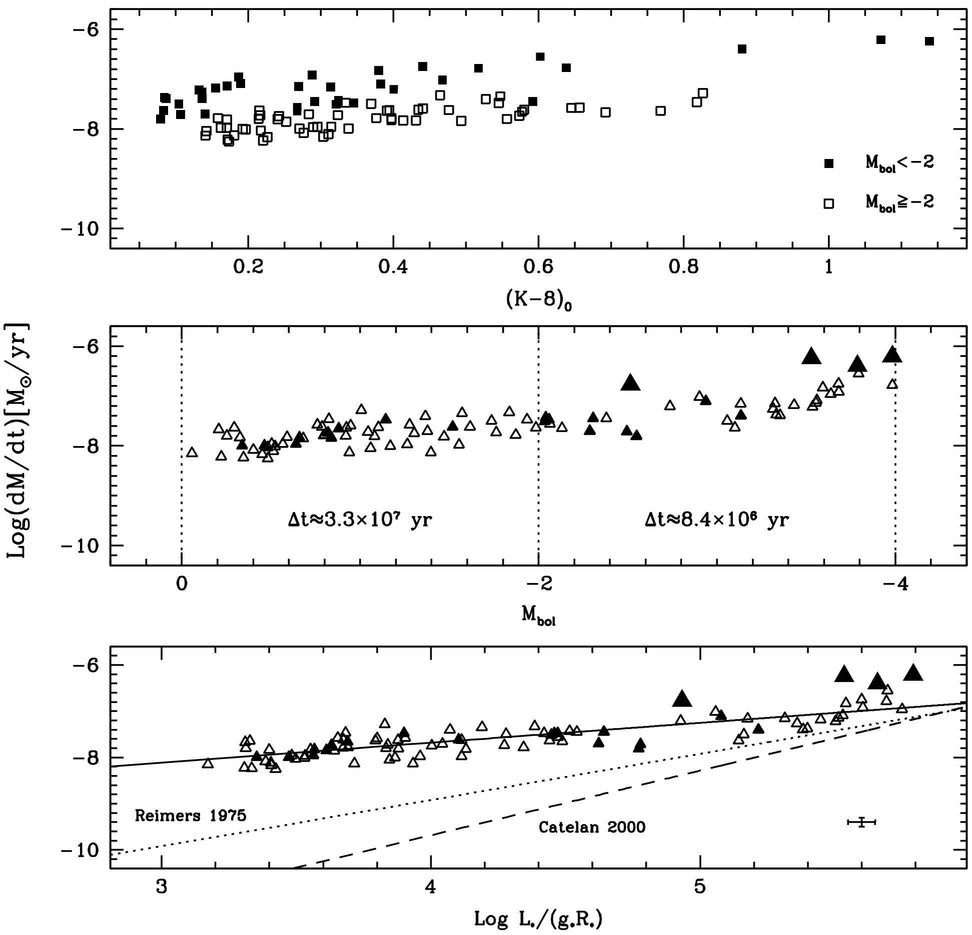

Fig. 4. ML rates for the SPITZER sources of 47 Tuc with dust excess, as a function of the observed $(K - 8)_0$ color (top panel), bolometric magnitude (middle panel) and normalized stellar luminosity (bottom panel). In the top panel stars with $M_{\rm bol} < -2$ and $M_{\rm bol} \geq -2$ are plotted as filled and open squares, respectively. In the middle and lower panels filled big triangles mark those giants which are known long period variables, filled small triangles are other AGB stars. In the middle panel the evolutionary timescale Δt in 2 luminosity intervals are also reported. In the bottom panel all of the AGB stars are excluded from the fit (solid lines). Typical random error bars are shown in the bottom right corner. The empirical laws by Reimers (1975a,b) with $\eta = 0.3$ (short-dashed line) and Catelan (2000) (long-dashed line) are also shown for comparison. From Origlia et al. (2007).

and $L_\odot$, $g_\odot$, and $R_\odot$ are the stellar luminosity, gravity and radius in solar units. In our study of 47 Tuc $C = 1$. Only true RGB stars are used to derive the fitting formula. The average random error on the inferred ML rates is ≈25%.

4. Discussion and conclusions

As shown in Fig. 4, our new ML law calibrated on Population II RGB stars is significantly flatter than the original Reimers formulation and the one revised by Catelan (2000), which have slopes of 1 and 1.4, respectively.

As we found in our ISOCAM survey, only a fraction of stars along the RGB are currently losing mass: ≈ 32% in the upper 2 mag, ≈ 16% down to the HB. This basically means that ML is "on" for only some fraction of the time, $f_{\rm on}$. By using a suitable evolutionary track for a RGB star of $M = 0.9\,M_\odot$ and $Z = 0.004$ (Pietrinferni et al. 2006), we can derive the evolutionary timescale Δt in each luminosity interval. Multiplying this by $f_{\rm on}$, we find that the timescale ML is "on" is less than a few Myr in each interval. By using the simple equation

$$\Delta M_{\rm RGB} = \Sigma_i \left(dM/dt_i \times \Delta t_i \times f_{{\rm on}_i}\right) \qquad (3)$$

we find that the total mass lost on the RGB is $\Delta M_{\rm RGB} \approx 0.23 \pm 0.07 M_\odot$.

Once the analysis of all the clusters in our survey will be finished, we will provide the first empirical ML law for Population II stars calibrated over a large range of metallicity, and investigating whether observed ML in individual stars within a cluster correlates with that cluster's HB morphology and if ML itself is involved in the second-parameter problem. Also, from the inferred duty cycles and intrinsic scatters, we should be able to shed some light on the driving ML mechanism, which is still quite unknown and matter of debate.

Acknowledgements. This work is based on observations made with the Spitzer Space Telescope, which is operated by the Jet Propulsion Laboratory, California Institute of Technology under a contract with NASA. Support for this work was provided by NASA through an award issued by JPL/Caltech. This research was supported by the Ministero dell'Istruzione, Università e Ricerca (MIUR), the PRIN-INAF 2006 and the Italian Space Agency (ASI).

References

Beccari, G., Ferraro, F. R., Lanzoni, B., & Bellazzini, M. 2006, ApJ, 652, 121
Boyer, M. L., Woodward, C. E., van Loon, J. Th., Gordon, K. D., Evans, A., Gehrz, R. D., Helton, L. A., & Polomski, E. F. 2006, AJ, 132, 1415
Cacciari, C., & Freeman, K. C. 1983, ApJ, 268, 185
Cacciari, C., Bragaglia, A., Rossetti, E., Fusi Pecci, F., Mulas, G., Carretta, E., Gratton, R. G., Momany, Y., & Pasquini, L. 2004, A&A, 413, 343
Castellani, M., & Castellani, V. 1993, ApJ, 407, 649
Catelan, M. 2000, ApJ, 531, 826
Clement, C. M. et al. 2001, AJ, 122, 2587
Cohen, J. G. 1976, ApJ, 203, 127
D'Cruz, N. L., Dorman, B., Rood, R.T., & O'Connell, R. W. 1996, ApJ, 466, 359
Dupree, A. K., Hartmann, L., & Avrett, E. H. 1984, ApJ, 281, 37
Dupree, A. K. 1986, ARA&A, 24, 377
Dupree, A. K., Sasselov, D. D., & Lester, J. B. 1992, ApJ, 387, 85
Dupree, A. K., Hartmann, L., Smith, G. H., Rodgers, A. W., Roberts, W. H., & Zucker, D. B. 1994, ApJ, 421, 542
Elitzur, M., & Ivezić, Z. 2001, MNRAS, 327, 403
Frogel, J. A., & Elias, J. H. 1988, ApJ, 324, 823
Fusi Pecci, F., & Renzini, A. 1975, A&A, 39, 413
Fusi Pecci, F., & Renzini, A. 1976, A&A, 46, 447
Fusi Pecci, F., et al. 1993, AJ, 105, 1145
Gillet, F. C., deJong, T., Neugebauer, G., Rice, W. L., & Emerson, J. P., 1988, AJ, 96, 116
Goldberg, L. 1979, QJRAS, 20, 361
Gratton, R.G. 1983, ApJ, 264, 223
Gratton, R. G., Pilachowski, C. A., & Sneden, C. 1984, A&A, 132, 11
Hansen, B. M. S. 2005, ApJ, 635, 526

Habing, H.J., Tignon, J., & Tielens, A.G.G.M. 1994, A&A, 286, 523

Kalirai, J. S. et al. 2007, ApJ, in press (astro-ph/07050977)

Ivezić, Z., Nenkova, M., & Elitzur, M., 1999, User Manual for DUSTY, (Lexington: Univ. Kentucky)

Judge, P.G., & Stencel, R. E. 1991, ApJ, 371, 357

Lyons, M. A., Kemp, S. N., Bates, B., & Shaw, C. R. 1996, MNRAS, 280, 835

Mauas, P.J.D., Cacciari, C., Pasquini, L. 2006, A&A, 454, 609

Mullan, D. J. 1978, ApJ, 226, 151

Netzer, N., & Elitzur, M. 1993, ApJ, 410, 701

Origlia, L., Ferraro, F. R., & Fusi Pecci, F. 1996, MNRAS, 280, 572

Origlia, L., Ferraro, F.R., Fusi Pecci, F., Rood, R.T. 2002, ApJ, 571, 458

Origlia, L., Rood, R. T., Fabbri, S., Ferraro, F. R., Fusi Pecci, F., Rich, R. M. 2007, ApJ, 667, 85

Pietrinferni, A. Cassisi, S., Salaris, M., Castelli, F. 2006, ApJ, 642, 797

Ramdani, A., & Jorissen, A. 2001, A&A, 372, 8

Reimers D. 1975a, in Problems in Stellar Atmospheres and Envelopes, eds. B. Baschek, W. H. Kegel, & G. Traving (Berlin: Springer), 229

Reimers D. 1975b, in *Mem. Soc. R. Sci. Liège 6 Ser.*, 8, 369

Renzini, A. 1977, in *Advanced Stages of Stellar Evolution*, ed. Bouvier & A. Maeder (Geneva Obs., Geneva), 151

Rood, R.T. 1973, ApJ, 184, 815

Schroeder, K. P., & Cuntz, M. 2005, ApJ, 630, 73

Smith, G. H., Dupree, A. K., & Strader, J. 2004, PASP, 116, 819

Willson, L. A. 2000, ARA&A, 38, 573